American Mineralogist, Volume 88, pages 493–500, 2003

O atom sites in natural kaolinite and muscovite: ^{17}O MAS and 3QMAS NMR study

SUNG KEUN LEE* AND JONATHAN F. STEBBINS

Department of Geological and Environmental Sciences, Stanford University, Stanford, California 94305, U.S.A.

ABSTRACT

The layer silicates are among the most common minerals in the Earth's surface environment, play important roles in many geological processes, and have diverse technological applications. While it has been suggested that O isotope exchange and dissolution kinetics in aqueous solutions are controlled by chemical bonding and local atomic structures, the effect of atomic environment around O atom sites in clay minerals on their site-specific reactivities with H_2O are not well known, mainly because direct experimental evidence is lacking.

Here, we present for the first time detailed high-resolution ^{17}O NMR data for ^{17}O-exchanged natural kaolinite [$Al_2Si_2O_5(OH)_4$] and muscovite [$KAl_2(AlSi_3)O_{10}(OH)_2$] using ^{17}O triple quantum magic angle spinning (3QMAS) and MAS NMR at high fields. At least two basal O atom sites in kaolinite are resolved: O4, and (O3 + O5). Apical O atoms ($^{[4]}$Si-O-2$^{[6]}$Al) and hydroxyl groups are also shown in these spectra. The ^{17}O 3QMAS spectrum for muscovite shows improved resolution over the ^{17}O MAS NMR spectrum, allowing us to resolve several basal O atoms, including ($^{[4]}$Si-O-$^{[4]}$Al), as well as hydroxyl groups. The fraction of each O atom appears to deviate somewhat from the stoichiometric value, suggesting that each crystallographically distinct site may have a different rate of exchange with the O atom in H_2O.

INTRODUCTION

The interaction between layer silicates and water has long been studied theoretically and experimentally because of its importance in O atom isotope exchange fractionation and geologic processes such as weathering and diagenesis (Savin and Lee 1988). Layer silicates have large surface areas and thus also have important applications to nuclear waste storage and industrial catalysis (Sposito et al. 1999).

Extensive macroscopic isotope exchange measurements and statistical thermodynamic analyses have suggested that the kinetics of isotope exchange and of dissolution may be strongly affected by average chemical bonding in specific silicate and oxide minerals (Cole and Ohmoto 1986; Savin and Lee 1988; Sverjensky 1992; Cole 2000). Some examples include faster O atom isotope exchange for minerals with more non-bridging O atoms (for example, chain silicates vs. tectosilicates) (Cole 2000). The rate-determining step of mineral dissolution is usually metal-O atom bond dissociation. Thus, dissolution behavior of specific minerals has been semi-quantitatively modeled using their relative average bond strengths (Sverjensky 1992; Lasaga 1995). Several theoretical approaches, including quantum chemical calculations, have revealed the importance of bonding environment and topology in the kinetics of mineral-fluid interactions, including kaolinite dissolution (Xiao and Lasaga 1994; Lee et al. 2001). Recent experimental studies including liquid-state ^{17}O NMR on a simple aqueous aluminum complex (Al_{13}) (Phillips et al. 2000), and solid state ^{17}O NMR on zeolites (Xu and Stebbins 1998; Stebbins et al. 1999; Cheng et al. 2000), have buttressed the theoretical results, revealing that each O atom site in these systems has a distinct reactivity (rate of exchange of O atoms) with H_2O.

Testing these results on more complex but more common minerals at the Earth's surface, such as clay minerals, is particularly important, because clays are among the most important indicators of geologic processes in the environment. This testing, however, is experimentally challenging and can be limited by the resolutions of spectroscopic and diffraction methods.

As has been previously demonstrated, element-specific solid-state ^{17}O NMR is one of the most effective and promising probes of O atom sites and their specific reactivities (Walter et al. 1988; Xu and Stebbins 1998; Lee et al. 2001), ^{17}O is, however, a quadrupolar nuclide. Interactions between the electric field gradient and the quadrupolar moments of the nuclei, combined with overlap in chemical shifts, often yield heavily broadened NMR spectra for O atom sites with similar environments in complex materials. As a result, there have been few ^{17}O NMR studies of clay minerals. Previous ^{17}O static NMR studies of talc [$Mg_3Si_4O_{10}(OH)_2$] combined with cross-polarization from protons revealed three O atom sites, including Si-O-Mg, Si-O-Si and Mg-OH, that have distinct ranges of structurally relevant NMR parameters, coupling constants (C_q), asymmetry parameter (η), and isotropic chemical shift (δ_{iso}), but ^{17}O static NMR has not allowed further resolution among O atom sites (Walter et al. 1988). A possible solution for achieving high resolution in solid-state NMR is magic-angle spinning (MAS) NMR at higher magnetic fields, which reduces the quadrupolar broadening (Stebbins et al. 2000). Further advances, such as triple-quantum magic-angle spinning (3QMAS) NMR at high fields, can provide much improved resolution, free from quadrupolar

* Geophysical Laboratory, Carnegie Institution of Washington, 5251 Broad Branch Rd., N.W, Washington, D.C. 20015. E-mail: s.lee@gl.ciw.edu

0003-004X/03/0004–493$05.00

broadening, in disordered solids including crystalline and amorphous silicates (Frydman and Harwood 1995; Stebbins et al. 1999; Lee and Stebbins 2000a; Lee and Stebbins 2000b; Lee and Stebbins 2002).

Here we report ^{17}O 3QMAS and MAS spectra for natural layer silicates such as kaolinite and muscovite at high field (14.1 and 18.8 Tesla). We also discuss relative reactivities of crystallographically distinct O atom sites in contact with aqueous solutions and the effect of these stabilities on macroscopic reactivity and O atom isotope exchange kinetics.

Experimental method

Sample preparation and characterization

150 mg of powdered muscovite from a pegmatite in Maine (Stanford University no. 62780) was sealed in a gold tube with an equal weight of 46% ^{17}O- enriched water and reacted at 773 K and 1 kbar for 1 month in a cold seal vessel. Standard Georgia kaolinite (KGa-1b, from the Clay Minerals Society, Source Clay Repository, hereafter kaolinite_Ga) was sieved to <20 μm and placed in a gold tube with the same weight of 46% ^{17}O-enriched water. The sample was then hydrothermally reacted at 573 K and 200 bar for 1 month, again in a cold seal vessel. After the reaction, the samples were dried at ambient temperature.

SEM of the two samples before and after reaction did not reveal obvious new phases formed during hydrothermal reactions within the resolution of the method, although the muscovite surface appeared to be somewhat altered. Powder XRD for the hydrothermally reacted kaolinite_Ga showed no impurity phases with a detection limit of about 5%. A MINTEQ (v.202) calculation for kaolinite shows that about 0.23 mol% of the initial sample could have been dissolved at 573 K and that the small volume of fluid could have been oversaturated with several other phases, including imogolite, which were not clearly detected by SEM and XRD in the reaction products. This calculation also suggested a drop in pH to about 3 may have occurred during the exchange experiment. ^{27}Al NMR spectra for kaolinite_Ga showed negligible differences for samples before and after hydrothermal isotope exchange.

NMR spectroscopy

^{17}O MAS NMR spectra for kaolinite were collected at three static magnetic fields with a modified Varian-VXR400S spectrometer (9.4 T) at a Larmor frequency of 54.2 MHz (5 mm Doty Scientific probe) and with Varian Inova 600 and Inova 800 spectrometers (14.1 T and 18.8 T) at Larmor frequencies of 81.3 and 108.4 MHz, respectively (3.2 mm Varian/chemagnetics T3 probes). The ^{17}O MAS NMR spectrum of muscovite was collected at 14.1 T. Relaxation delay was 1 sec for each sample with spinning speeds of 15, 18, and 20 kHz at 9.4, 14.1, and 18.8 T, respectively. Radio frequency pulse lengths of 0.25 to 0.3 μs were used at each field, corresponding to about a 15° tip angle for the central transition in solids. The spectra are referenced to ^{17}O-enriched water, or tap water. The ^{17}O 3QMAS NMR spectra for kaolinite and muscovite were collected using a FAM-based (fast amplitude modulation) shifted-echo pulse sequence (See Zhao et al. 2001 and references therein) comprising hard pulses with durations of 3 and 0.7 μs, and a selective pulse with a duration of 20 μs at 14.1 T. The spinning speed was 18 kHz. ^{17}O 3QMAS NMR spectra for muscovite at 9.4 T were collected with the shifted-echo pulse sequence comprising two hard pulses of duration 5.2 μs and 1.7 μs, and a selective pulse with duration of 26 μs with sample spinning speed of 15 KHz. Typically, signal averaging for about 2 (muscovite) to about 10 days (kaolinite) was required to obtain the 3QMAS spectra shown.

Comparing hydrothermally enriched kaolinite with clay minerals of similar composition synthesized with ^{17}O (Lee et al., in preparation), the ratio of signal intensities (synthetic/hydrothermal enrichment) in the ^{17}O MAS NMR spectra at 9.4 T is about 2 to 4. Here both spectra were collected at recycle delays of three times the spin-lattice relaxation times for muscovite and kaolinite, which are about 1 and 2.5 s respectively. Because the intensity ratio reflects the relative amounts of ^{17}O in the samples, this strongly suggests that there is significant bulk exchange in addition to the exchange at terminal (surface) O atom sites. The published surface area for KGa-1B kaolinite, determined by the Brunauer-Emmett-Teller (BET) method, is 11.1 ± 0.4 m^2/g (Ganor et al. 2001), which leads to a ratio of bulk/surface (edge) oxygen of about 70, confirming that O atom site exchange was prominent not only on edge and surface sites but also in the bulk.

Results and discussion

^{17}O MAS and 3QMAS NMR results

Kaolinite, which is one of the simplest clay minerals, has three crystallographically distinct basal O atom sites with equal populations, two apical O atoms (O1 and O2) linking tetrahedral and octahedral layers with identical site fractions, and four hydroxyl groups (Fig. 1). The environments of the three basal O atoms (O3, O4, and O5) are chemically similar with little variation in Si-O bond length and Si-O-Si bond angle. Among the four hydroxyl groups, OH4 is located between the octahedral and tetrahedral layers, and the others face basal O atoms in the adjacent tetrahedral layer, forming weak hydrogen bonds. Atomic configurations around the two crystallographically distinct apical O atoms (O1 and O2) are rather similar. Bond angles and lengths around each O atom site vary slightly among different structural refinements. For example, Neder et al. reported Si-O-Si angles for O3, O4, and O5 of 130.1°, 141.8°, and 130.4°, respectively (Neder et al. 1999), while those from Bish and Von Dreele (1989) are 130.6°, 142.5°, and 131.4°, respectively. Muscovite, which can be regarded as a model system for 2:1 dioctahedral clay minerals including illite, has three basal O atoms, two apical O atom sites with equal populations, and one hydroxyl group.

Figure 2 illustrates ^{17}O MAS spectra of hydrothermally exchanged kaolinite_Ga at varying magnetic fields (9.4, 14.1, and 18.8 T) and muscovite at 14.1 T, demonstrating the effect of static field on resolution and spectral broadening. Hydrothermal reactions allow exchange of O atom isotopes between the original silicates (^{16}O) and fluids (^{17}O, NMR active). Therefore essentially all NMR signal intensity represents the O atom in sites that have exchanged with ^{17}O-enriched water. Because

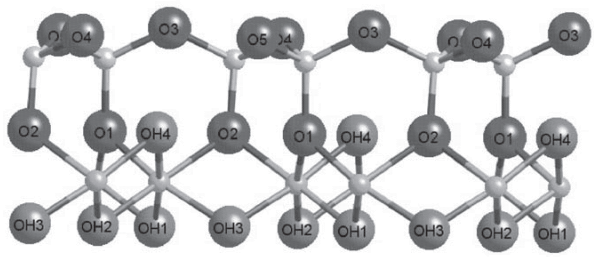

FIGURE 1. O atom sites in kaolinite. Basal O atom sites are O3 [Si-O-Si(IV)], O4 [Si-O-Si(III-1)], and O5 [Si-O-Si(III-2)]. Two apical O atom sites are O1 and O2 that can be either Si-O-2$^{[6]}$Al(I) or Si-O-2$^{[6]}$Al(II) in Figures 4, 5 and 7. OH1 through OH4 refer to hydroxyl groups.

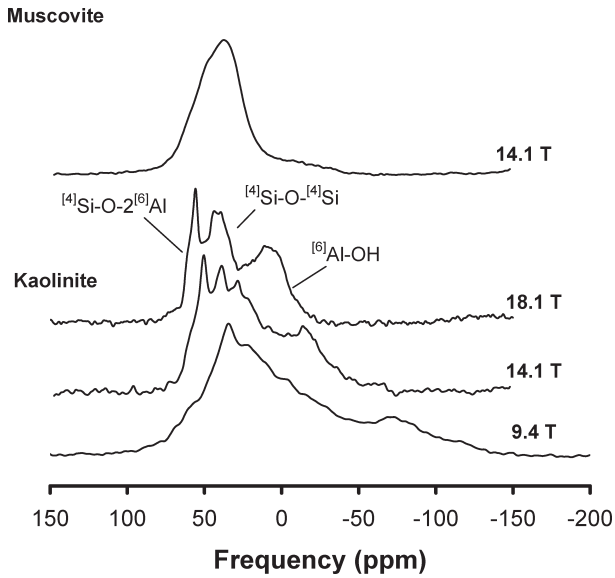

FIGURE 2. ^{17}O MAS NMR spectra for ^{17}O-exchanged natural muscovite and kaolinite at 9.4, 14.1, and 18.8 T.

differences in equilibrium isotope partitioning among different sites are expected to be too small to be detectable (at most a few percent) at the typical precision level of NMR measurement, variation from stoichiometry in the observed relative intensities for O atoms at different sites reflects the extent of reaction between the sites and the fluids, potentially allowing quantitative assessment of site-specific stabilities. Basal ($^{[4]}$Si-O-$^{[4]}$Si) and apical ($^{[4]}$Si-O-2$^{[6]}$Al) O atom sites and hydroxyl groups in kaolinite are resolved at 18.8 T. The assignments of hydroxyl groups and basal O atoms are based on previous studies of crystalline aluminosilicates (Walter et al. 1988; Xu et al. 1998; van Eck et al. 1999), while the peak centered around 50 ppm at 14.1 T for kaolinite was assigned as apical O atoms. On the other hand, closely related but crystallographically distinct sites such as different basal O atom sites are not well resolved even at one of the highest fields currently available (18.8 T). ^{17}O MAS spectra for the hydrothermally exchanged muscovite are broadened, probably because of the presence of paramagnetic impurities including Fe, a common substitution for Al in the octahedral layer among natural samples. Thus these spectra do not provide explicit information on O atom sites.

Clay minerals often show preferred orientation in XRD experiments, and silicates such as Na_2SiO_3 that cleave into thin needles have been shown to produce distorted quadrupolar line shapes when packed into the narrow ceramic rotors used for MAS NMR (George 1997; George et al. 1998). To check the effect of preferred orientation on the kaolinite MAS spectrum, we collected data at 14.1 T for a mixture of coarse, granular SiO_2 (about 60 wt%) and kaolinite (about 40 wt%). In this two-phase mechanical mixture, some fraction of kaolinite powder coats the surfaces of the SiO_2 particles, while much is trapped between large particles and thus is not compressed during sample packing, which ensures a further deviation from preferred orientation. As shown in Figure 3, there is negligible difference in the spectrum for kaolinite compared to that of the mixture, which implies that kaolinite particles do not have strong preferred orientation, possibly due to their small size.

Figure 4 shows the ^{17}O 3QMAS NMR spectrum of kaolinite, which provides improved resolution for apical and basal O atoms as well as hydroxyl groups. At least two types of basal O atoms [assigned to O4 and (O3 + O5) on the basis of similarities in bond angles] are resolved in the spectra, as is the distinction between apical and basal O atoms (Fig. 4a). O3 and O5 may also be partially resolved due to a small difference in chemical shifts. The two types of apical O atoms, namely $^{[4]}$Si-O-2$^{[6]}$Al(II) and $^{[4]}$Si-O-2$^{[6]}$Al(I) are not clearly resolved in this spectrum: the shoulder at –40 ppm (isotropic dimension) may be due to incomplete overlap of these two sites. Hydroxyl groups are less likely to be observed in 3QMAS NMR experiments because of the likelihood of short spin-spin relaxation times and their relatively large quadrupolar coupling constants, C_q, of 6.5–7 MHz (van Eck et al. 1999; Lee and Stebbins 2000b; Lee et al. in preparation). However, some OH may be detectable partly because of its high mole fraction of 44.4%, as represented by the broad feature at –25 ppm shown in Figure 4b.

Figure 5a shows the isotropic projection (sum of data along

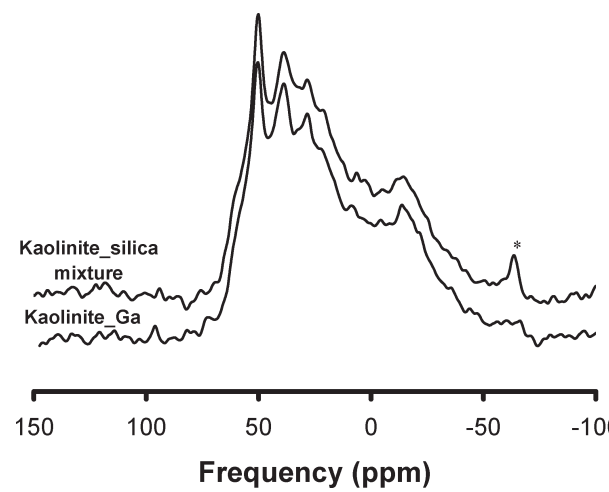

FIGURE 3. ^{17}O MAS NMR spectra for natural kaolinite and kaolinite + silica mixture at 14.1 T. * shows a spinning side band of the ZrO_2 rotor.

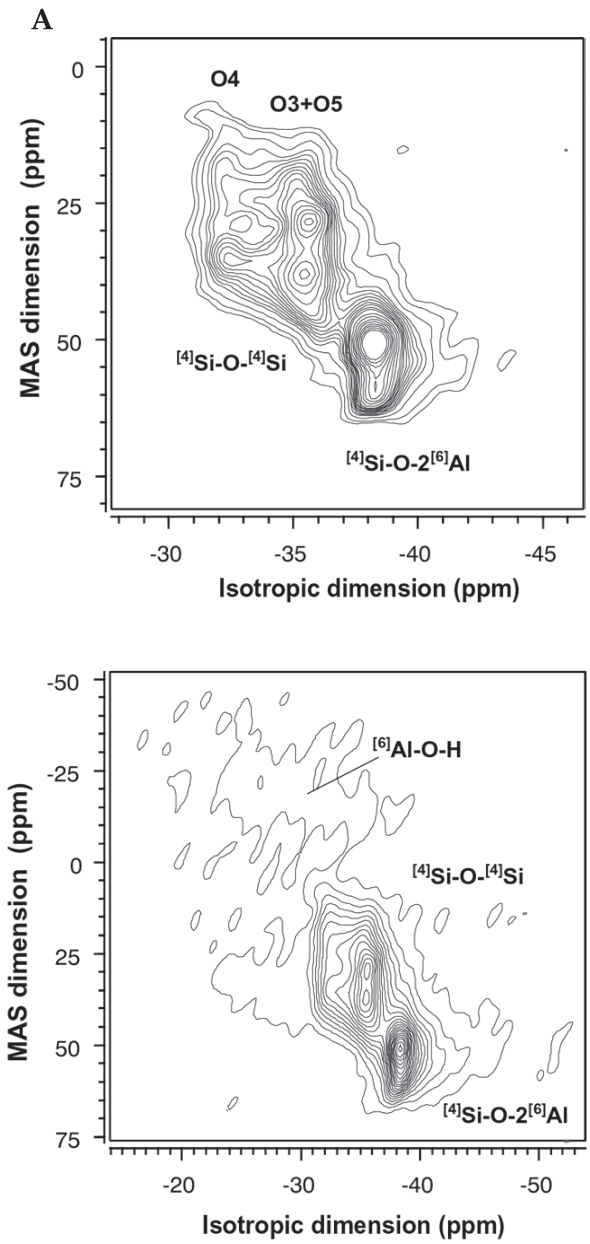

FIGURE 4. ^{17}O 3QMAS NMR spectrum for kaolinite collected at 14.1 T. (**a**) Contour lines are drawn from 10% to 80% of relative intensity with a 5% increment with the addition of contours at 7, 22.5, 27.5, 32.5, and 37.5 % to accentuate basal O atoms and low intensity features. (**b**) Same spectrum with more apodization (smoothing). Contour lines are drawn from 10% to 95% of relative intensity with a 5% increment, with a contour at 3% added to show hydroxyl group ($^{[6]}$Al-O-H) signal.

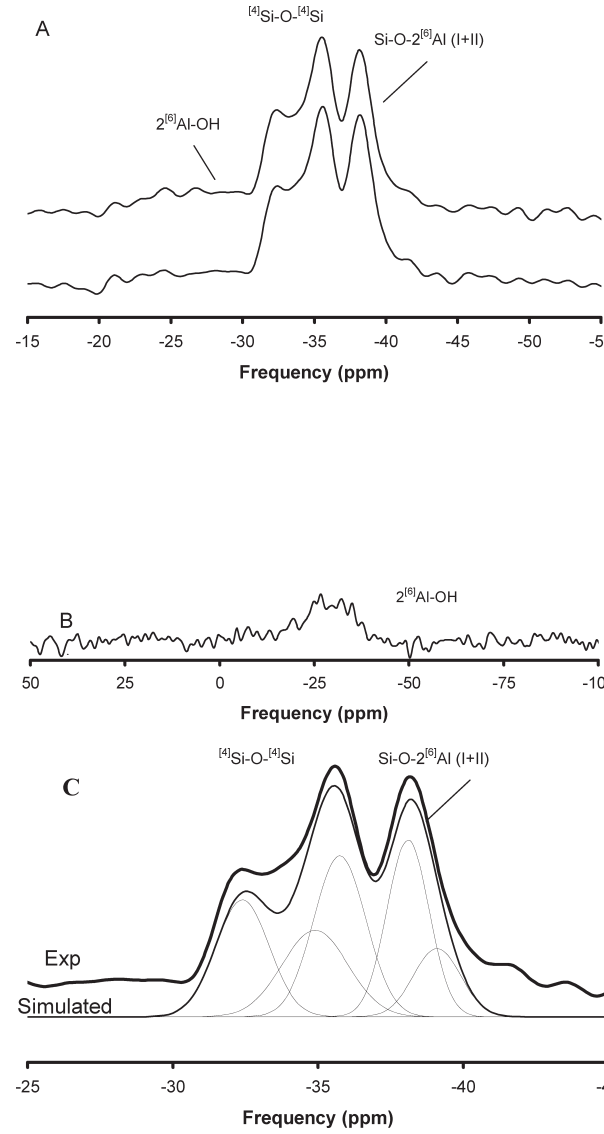

FIGURE 5. Isotropic projections of ^{17}O 3QMAS NMR spectrum for kaolinite collected at 14.1 T. (**a**) Upper plot: data with MAS positions from 70 to –50 ppm (entire data set shown in Fig. 4b); lower part from 70 to 5 ppm (approximate range of data shown in Fig. 4a). (**b**) Projection of data with MAS position from 5 to –50 ppm to isolate part of signal from hydroxyl groups. (**c**) Fitting result of the isotropic projection using three Gaussian peaks for basal O atom and two for apical O atoms.

lines parallel to the MAS axis) of the ^{17}O 3QMAS NMR spectrum where at least two types of basal O atoms and apical O atoms are clearly resolved. If the projection from 70 to –50 ppm in the MAS dimension (upper) is compared with that from 70 to 5 ppm (lower), signals from hydroxyl O atoms can also be seen, as also shown by the projection from –50 ppm to 5 ppm (Fig. 5b).

Intensity in 3QMAS NMR spectra is not quantitative and is mainly dependent on the magnitude of C_q (Medek et al. 1995; Lee and Stebbins 2000b). On the other hand, the relative intensity among different basal O atoms or among apical O atoms can be semi-quantitative due to the similar C_qs within each group (about 4.4–4.8 MHz for basal O atoms and 3.5 MHz for apical O atom sites). To attempt to estimate the contributions from crystallographically distinct sites within each of these groups, the isotropic projection was simulated with five Gaussian peaks

TABLE 1. ^{17}O NMR parameters for kaolinite and muscovite obtained from ^{17}O 3QMAS NMR and ^{17}O MAS NMR

maolinite	C_q (MHz)	δ_{iso} (ppm)	η	Intensity*(%)
$^{[4]}$Si-O-$^{[4]}$Si(IV) : O3	4.45 (±0.2)	54.3 (±1)	0.43 (±0.1)	14 (±3.5)
$^{[4]}$Si-O-$^{[4]}$Si(III-1) : O5	4.65 (±0.2)	51.3 (±1)	0.38 (±0.1)	12 (±3)
$^{[4]}$Si-O-$^{[4]}$Si(III-2) :O4	4.75 (±0.2)	46.5 (±1)	0.28 (±0.1)	8 (±3)
Hydroxyl group	6.9 (±0.4)	41.5 (±4)	0.55 (±0.15)	46 (±3.5)
$^{[4]}$Si-O-2$^{[6]}$Al(II)	3.4 (±0.1)	64.0 (±1)	0.8 (±0.05)	14 (±3)†
$^{[4]}$Si-O-2$^{[6]}$Al(I)	3.5 (±0.1)	65.0 (±1)	0.8 (±0.05)	6 (±3)†
muscovite	C_q	δ_{iso}	η	Intensity‡(%)
$^{[4]}$Si-O-$^{[4]}$Si	4.6 (±0.3)	53.0 (±3)	0.5 (±0.2)	20 (±3)
$^{[4]}$Si-O-2$^{[6]}$Al(I+II)	3.5 (±0.2)	66.5 (±2)	0.8 (±0.1)	33 (±3)
$^{[4]}$Si-O-$^{[4]}$Al	3.1 (±0.3)	46.2 (±3)	0.5 (±0.2)	30 (±3)
Hydroxyl group	6.75 (±0.5)	44.5 (±3)	0.5 (±0.2)	17(±3)

Notes: These results given here may not be unique due to overlap of peaks as well as C_q dependence of 3QMAS efficiency (see text).
* Stochiometric values for kaolinite are 11.1% for each basal (total of 33.3%) and apical oxygen (total of 22.2%) and 44.4% for all hydroxyl groups. Those for muscovite are 50, 33, and 17% for basal, apical, and hydroxyl groups.
† Fractions are from fits to the isotropic projection of the ^{17}O 3QMAS NMR spectrum at 14.1 T (Fig. 6) with calibration of the effect of C_q on intensity, as discussed previously (Lee and Stebbins 2000b). Fraction of hydroxyl groups is from fitting the lower frequency shoulder of the ^{17}O MAS NMR spectrum (Fig.1).
‡ Due to unresolved nature of the two apical O atoms in the ^{17}O MAS NMR spectrum, the fractions are from fitting result of isotropic projection of 3QMAS NMR spectra as given in Figure 5C.

(Fig. 5c). Peak intensities, widths, and positions were adjusted manually to avoid problems of noisy baselines with guidance from the frequencies and shapes of features in the full 2D data sets. Although results of this process are not unique, they suggest that ^{17}O-exchanged fractions of O atoms in the three basal sites may not be equal; a similar result is suggested for the apical O atoms. MAS dimension "slices" of the 2D data, taken at the position of fitted Gaussians, were analyzed to estimate corresponding values of δ_{iso} and P_q [$= C_q\,(1 + \eta^2 / 3)^{1/2}$, where $0 \le \eta \le 1$ is the quadrupolar asymmetry parameter]. These values, and in some cases relative peak areas, were used (see below) to constrain fits of the MAS spectra, which in principle have more quantitative areas.

As shown in MAS and 3QMAS NMR spectra, apical O atoms are more deshielded (higher frequency, left side as plotted in MAS spectra) than basal O atoms. In addition, the three basal O atom sites suggested by the 3QMAS NMR spectra have different degrees of shielding and thus different chemical shifts as well as differences in C_q (See Table 1 and below for discussion). ^{17}O NMR peak assignments within each group are not trivial, because the local atomic configurations are similar and the relations between the atomic environment and ^{17}O NMR parameters, such as δ_{iso} and C_q, are not well known. C_q for ^{17}O has usually been shown to increase with increasing Si-O-Si bond angle (Grandinetti et al. 1995; Vermillion et al. 1998), but this correlation was not clearly shown in recent NMR and quantum simulation studies of some zeolites (Bull et al. 2000). Here, if we use this correlation, the basal O atom site with the largest C_q (4.75 MHz) may be assigned to O4 and the other sites with smaller C_q values may be assigned to O3 and O5 (Table 1).

^{17}O 3QMAS NMR spectra for muscovite are also shown in Figure 6, where two types of basal O atom sites, $^{[4]}$Si-O-$^{[4]}$Si and $^{[4]}$Si-O-$^{[4]}$Al, as well as $^{[4]}$Si-O-2$^{[6]}$Al are resolved, thus being much more informative than the MAS NMR spectrum (Fig. 2). A small fraction of hydroxyl O atoms are also observed centered at about –35 and –15 ppm in 3QMAS and MAS dimensions respectively. The peak position is close to that calculated from NMR parameters from simulation of MAS NMR data (about –37.5 and –6 ppm in the 3QMAS and MAS dimensions), which is also similar to the peak position predicted from the NMR parameters of bayerite [$Al(OH)_3$]: C_q, δ_{iso}, and η are 6 MHz, 40 ppm, and 0.3 respectively, which leads to –32.8 and –6.3 ppm in the 3QMAS and MAS dimensions (Walter and Oldfield 1989).

Simulation results and implications

As mentioned above, quantification of O atom sites in these two samples from 3QMAS NMR can be complicated by many factors (Medek et al. 1995; Lee and Stebbins 2000b) but can be improved by simulating MAS spectra using NMR parameters from 3QMAS NMR spectra. Figure 7 shows the results of the simulation (again done by iterative, manual adjustment of parameters) of the ^{17}O MAS NMR spectrum of kaolinite at 14.1 T where signals from the six crystallographic sites can be separated. C_q, δ_{iso}, and η of each site are given in Table 1. It should be noted that these results are not unique and thus the simulation result given here is one of a set of possible solutions. As previously mentioned, peak assignment is also not trivial, especially for apical O atoms that have similar atomic configuration as well as similar C_q and δ_{iso}. These two peaks can be either O1 or O2. As shown in Table 1, the C_q of basal O atoms appears to increase with decreasing δ_{iso} and η. Future quantum chemical calculation for large O atom clusters, that include effects beyond the first coordination shell, and further ^{17}O NMR on crystalline silicates may be helpful to refine assignment. For example, a recent ^{17}O NMR study of chain silicates reports correlation between Si-O and δ_{iso}, where deshielding increases with increasing Si-O distance (Ashbrook et al. 2002).

The ^{17}O NMR intensity of each peak may reflect the extent of exchange with $H_2{}^{17}O$ and thus the rate of reaction of each O atom site in contact with aqueous fluids. Due to the inherent uncertainty in simulation results caused by overlap of the six peaks, it is impossible to draw any definite conclusions from the data given above (Fig. 7). First, the ratios of the fractions

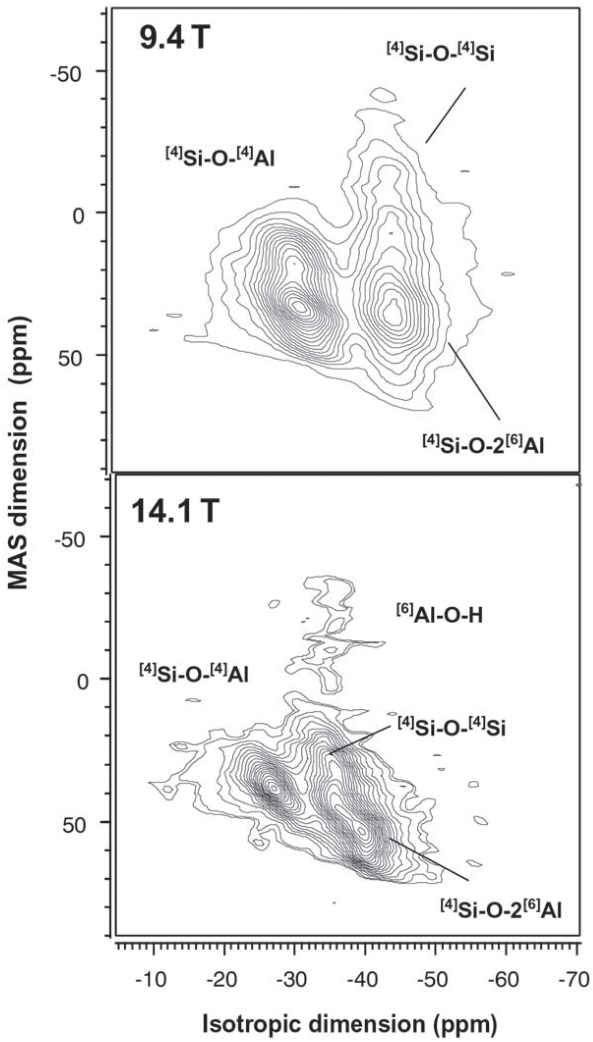

FIGURE 6. ^{17}O 3QMAS NMR spectra for muscovite at 9.4 and 14.1 T. Contour lines are drawn from 4% to 99% of relative intensity with a 5% increment.

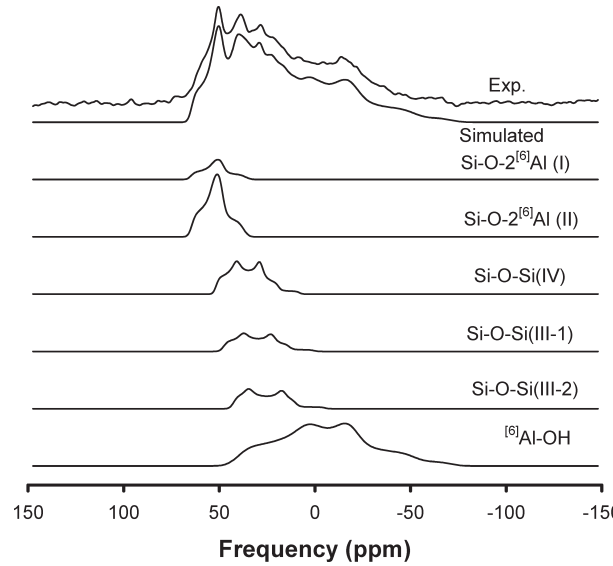

FIGURE 7. Simulation results for ^{17}O MAS NMR spectrum for kaolinite at 14.1 T (**top**). Simulated component peaks are shown below, using the C_q and δ_{iso} from 3QMAS NMR as initial parameters (Table 1).

of total basal O atoms : apical O atoms : hydroxyl group appear to be close to those predicted by stoichiometry (3:2:1) and equal reactivity (or that equilibrium was obtained). On the other hand, the fraction of (O3 + O5)/O4 from the MAS NMR simulation appears to be somewhat larger than the prediction of 2 (Table 1); O3 and O5 have smaller Si-O-Si angles (Bish and Von Dreele 1989; Neder et al. 1999) and may have greater reactivity than O4 with an Si-O-Si angle of 141°. The apparent reactivity difference may result from the fact that the relative energy of the [4]Si-O-[4]Si cluster is a function of bond angle, and the lattice stability decreases with increasing deviation from the equilibrium [4]Si-O-[4]Si angle of about 144° (Lee et al. 2001). On the other hand, the similar fraction of O5 and O4 (but smaller than O3) can also lead to a relatively good simulation results, implying that the assignment may not be unique. The other possible reason may be the hydrogen bonds between basal O atoms and the protons in hydroxyl groups in octahedral layers (Neder et al. 1999; Benco et al. 2001). These hydrogen bonds probably selectively decrease the probability of the protonation of basal O atoms, depending on the configuration of hydrogen atoms around basal O atoms. However, the O-H···O distance of each basal O atom in kaolinite is similar (2.21–2.35 Å), and thus this may not be a primary reason (Neder et al. 1999; Benco et al. 2001). A reactivity difference in basal O atoms has previously been assumed in Monte Carlo simulations of kaolinite dissolution, where multiple rate constants were modeled for each basal O atom with different topology and varying number of reactive sites near these O atoms (Lasaga 1995).

The fraction of the two types of apical O atoms is especially difficult to quantify due to the overlap between their two peaks in ^{17}O NMR spectra as well as their similar atomic configuration. As shown in Table 1, the [4]Si-O-2[6]Al(II)/[4]Si-O-2[6]Al(I) fraction of about 2.5 is apparently larger than predicted value of 1 if we include the shoulders in the ^{17}O 3QMAS NMR spectrum of kaolinite (Fig. 5c). However, it should be noted that this assignment is again not unique and requires more experiments with varying reaction times for confirmation. NMR at even higher field may also be helpful. On the other hand, it would not be surprising to observe differential O atom site fractions that deviate from the equilibrium values. Distinct hydroxyl O-atom sites with similar atomic environments in the aqueous Al_{13} molecule also have shown significant variations in reactivity (Phillips et al. 2000). The considerable fraction of apical O atom sites suggests that direct protonation of these O atoms is favorable, as recently suggested for kaolinite dissolution (Nagy 1995; Ganor et al. 2001). It is also worthwhile to mention that recent quantum chemical calculations show hydrogen diffusion into bulk solids, which could allow protonation of apical O atoms that are not exposed at an edge site (Sohlberg et

al. 1999). H isotope exchange is much more efficient than that of O atoms, as has been demonstrated by rapid H isotope exchange (Savin and Lee 1988). As previously mentioned, surface O atom exchange alone cannot account for the observed ^{17}O NMR total intensity. Direct H_2O or H diffusion in layer silicates is more likely due to larger cavities in both octahedral and tetrahedral layers as well as interactions at edge sites, as inferred from the significant intensity of apical O atoms and in particular basal O atoms in the NMR spectra for kaolinite.

Due to the severe quadrupolar broadening from their large C_q values, hydroxyl groups are not resolved. However, differential reactivity among hydroxyl groups may be prominent as shown for the Al_{13} molecule (Phillips et al. 2000) because OH(I-III) sites have different bonding environments than OH(IV) sites (Fig. 1). Although further resolution could be achieved at higher fields, the fraction of two basal O atoms $^{[4]}$Si-O-$^{[4]}$Al/$^{[4]}$Si-O-$^{[4]}$Si in muscovite (≈1.5) is apparently larger than 1, the value predicted from the homogeneous distribution of Si/Al and equal reactivity in the tetrahedral layer. This suggests that reactivity of $^{[4]}$Si-O-$^{[4]}$Al clusters may be greater than that of $^{[4]}$Si-O-$^{[4]}$Si in tetrahedral layers, consistent with recent results from zeolites (Xu and Stebbins 1998; Cheng et al. 2000) and from quantum chemical calculation showing a lower activation energy barrier for Si-O-Al (Xiao and Lasaga 1994). The Al-O-Al cluster, which has implications for the extent of disorder among tetrahedral cations, was not detected, implying that the distribution of Al in tetrahedral layers appears to obey the homogeneous distribution of charge, or the Al avoidance rule (Lee and Stebbins 1999).

The above experimental results may thus show the effects of structure and chemical bonding environment within a single crystal on the reactivity of each site as well as on macroscopic reactivity, and may explain the origin of multiple exponential behavior in the temporal variation of O atom isotope exchange ratios found in many minerals, including layer silicates, quartz, carbonates, and zeolites (Criss et al. 1987; Xu et al. 1998). A bi-exponential approach, using two exponentials to represent fast and slow exchange, has been used to analyze the variation of O atom isotope exchange with time (Criss et al. 1987). On the other hand, Figure 8 shows the hypothetical exchange fraction of kaolinite with time, using a multi-rate, site dependent model where each O atom site has distinct first-order exchange rate with water. Here we further assume that the site fractions observed in this study may reflect the relative magnitude of the forward rate constant. For example, the rate constant of basal O atoms ($K_{Si\text{-}O\text{-}Si}$) is smaller than that of hydroxyl group ($K_{Al\text{-}O\text{-}H}$).

The superposition of each first-order kinetic solution, scaled with the stoichiometric fraction of each O atom site, leads to bulk data that certainly deviate from first order exchange kinetics. The results suggest that the superposition of simple first-order exchange kinetics for each O atom site, tied to their relative reactivity, can partly account for macroscopic experimental results where the information for all O atom sites is averaged together. Unfortunately, a quantitative reaction model cannot be obtained from our present observations because of a limited data set and the fact that exchange kinetics are a function of many variables, including surface area and diffusion of water as well as experimental conditions (Cole and Ohmoto 1986; O'Neil 1986; Cole 2000).

This site-specific reactivity also has important implications for dissolution kinetics at surfaces, in that small variations in chemical environment and topology can lead to significant differences in reactivity, as has recently been demonstrated (Hochella and Banfield 1995; Lasaga 1995; Phillips et al. 2000). The mechanism of O atom isotope exchange in a hydrothermal experiment may include Ostwald ripening by dissolution and precipitation, which should yield a crystal with identical O atom isotope fractionation (Stoffregen 1996) since the fractionation coefficient (k) for $^{17}O/^{16}O$, mainly controlled by the effective mass difference, is close to 1, which is somewhat different from our experimental data suggesting different O atom site exchange for basal O atoms. It is possible that the results shown here could result from a combination of both direct O atom exchange without further dissolution and possible dissolution and recrystallization (Stoffregen 1996), although no clear evidence of newly formed phases was found within the resolution of the XRD and SEM data. HRTEM can be potentially useful to characterize the possible alteration products, whose length scale can be a few nanometers (Hochella and Banfield 1995). Although uncertainties both in the nature of exchange process and in the data analysis preclude any quantitative conclusion on the reactivity of each O atom site, we have attempted here to provide a qualitative explanation for results that appear to deviate from the stoichiometric exchange at each O atom site, in particular for basal O atoms.

In general, a more rigorous description of the macroscopic kinetic properties of layer silicates in contact with aqueous solutions can be obtained from detailed atomic scale information on reactivity, and ^{17}O NMR can be helpful to shed light on a more complete, atomic-level understanding of the geological processes at the Earth's surface, including weathering and clay mineral diagenesis.

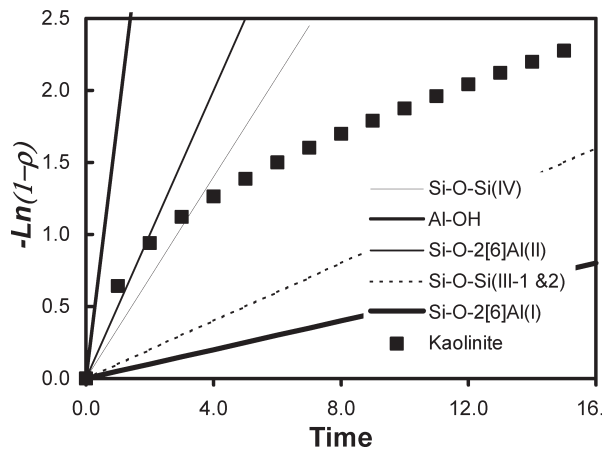

FIGURE 8. Hypothetical O atom site-specific reactivity of kaolinite. ρ is the apparent reactivity defined as the fraction of O atoms exchanged. Solid lines refer to the temporal variation of –ln(1 – ρ) for each O atom and closed square refers to the macroscopic reactivity variation of bulk kalolinite. The units of time and reactivity in the plot are arbitrary: quantitative rate constant cannot be obtained from the data here.

ACKNOWLEDGMENTS

This project was supported by a Stanford Graduate Fellowship and NSF grant no. EAR0104926. We thank J. Oglesby and G. Ernst for help in hydrothermal experiments and P. Zhao and Z. Xu for pulse sequence development. We also thank D.K. Bird and G.E. Brown Jr. for critical comments and helpful suggestions, and an anonymous reviewer and S. Kohn for helpful comments on the original manuscript.

REFERENCES CITED

Ashbrook, S.E., Berry, A.J., and Wimperis, S. (2002) O-17 multiple-quantum MAS NMR study of pyroxenes. Journal of Physical Chemistry B, 106, 773–778.

Benco, L., Tunega, D., Hafner, J., and Lischka, H. (2001) Upper limit of the O-H···O hydrogen bond. Ab initio study of the kaolinite structure. Journal of Physical Chemistry B, 104, 10812–10817.

Bish, D. and Von Dreele, R.B. (1989) Rietveld refinement of non-hydrogen atomic positions in kaolinite. Clays and Clay Minerals, 37, 289–296.

Bull, L.M., Bussemer, B., Anupold, T., Reinhold, A., Samoson, A., Sauer, J., Cheetham, A.K., and Dupree, R. (2000) A high-resolution O-17 and Si-29 NMR study of zeolite siliceous ferrierite and ab initio calculations of NMR parameters. Journal of the American Chemical Society, 122, 4948–4958.

Cheng, X., Zhao, P.D., and Stebbins, J.F. (2000) Solid state NMR study of oxygen site exchange and Al-O-Al site concentration in analcime. American Mineralogist, 85, 1030–1037.

Cole, D.R. (2000) Isotopic exchange in mineral-fluid systems. IV. The crystal chemical controls on oxygen isotope exchange rates in carbonate-H_2O and layer silicate-H_2O systems. Geochimica et Cosmochimica Acta, 64, 921–931.

Cole, D.R. and Ohmoto, H. (1986) Kinetics of isotopic exchange at elevated temperatures and pressures. In J.W. Valley, J.H.P. Taylor, and J.R. O'Neil, Eds., Stable Isotopes in High Temperature Geological Processes, p. 41–90. Mineralogical Society of America, Washington, D.C.

Criss, R.E., Gregory, R.T., and Taylor, H.P. (1987) Kinetic-theory of oxygen isotopic exchange between minerals and water. Geochimica et Cosmochimica Acta, 51, 1099–1108.

Frydman, I. and Harwood, J.S. (1995) Isotropic spectra of half-integer quadrupolar spins from bidimensional magic-angle-spinning NMR. Journal of the American Chemical Society, 117, 5367–5368.

Ganor, J., Sharon, N., and Jordi, C. (2001) The effect of kaolinite on oxalate (bio) degradation at 25 degrees C, and possible implications for adsorption isotherm measurements. Chemical Geology, 177, 431–442.

George, A.M. (1997) The structure and dynamics of the non-network forming elements sodium and magnesium in glassy and molten silicates: a high temperature NMR study. 110p, Ph.D. thesis, Stanford University.

George, A.M., Richet, P., and Stebbins, J.F. (1998) Cation dynamics and premelting in lithium metasilicate (Li_2SiO_3) and sodium metasilicate (Na_2SiO_3): A high-temperature NMR study. American Mineralogist, 83, 1277–1284.

Grandinetti, P.J., Baltisberger, J.H., Farnan, I., Stebbins, J.F., Werner, U., and Pines, A. (1995) Solid-state ^{17}O Magic-angle and dynamic-angle spinning NMR study of the SiO_2 polymorph coesite. Journal of Physical Chemistry, 99, 12341–12348.

Hochella, M.F. and Banfield, J.F. (1995) Chemical weathering of silicates in nature: a microscopic perspective with theoretical consideration. In A.F. White and S.L. Brantley, Eds., Chemical Weathering Rates of Silicate Minerals, p. 353–406. Mineralogical Society of America, Washington D.C.

Lasaga, A.C. (1995) Fundamental approaches in describing mineral dissolution and precipitation rates. In A.F. White and S.L. Brantley, Eds., Chemical Weathering Rates of Silicate Minerals, p. 23–86. Mineralogical Society of America, Washington D.C.

Lee, S.K. and Stebbins, J.F. (1999) The degree of aluminum avoidance in aluminosilicate glasses. American Mineralogist, 84, 937–945.

——— (2000a) Al-O-Al and Si-O-Si sites in framework aluminosilicate glasses with Si/Al=1: quantification of framework disorder. Journal of Non-Crystalline Solids, 270, 260–264.

——— (2000b) The structure of aluminosilicate glasses: High-resolution ^{17}O and ^{27}Al MAS and 3QMAS NMR study. Journal of Physical Chemistry B, 104, 4091–4100.

——— (2002) The extent of inter-mixing among framework units in silicate glasses and melts. Geochimica et Cosmochimica Acta, 66, 303–309.

Lee, S.K., Musgrave, C.B., Zhao, P., and Stebbins, J.F. (2001) Topological disorder and reactivity of borosilicate glasses: Ab initio molecular orbital calculations and ^{17}O and ^{11}B NMR. Journal of Physical Chemistry B, 105, 12583–12595.

Medek, A., Harwood, J.S., and Frydman, L. (1995) Mulitple-quantum magic-angle spinning NMR: a new method for the study of quadrupolar nuclei in solids. Journal of the American Chemical Society, 117, 12779.

Nagy, K.L. (1995) Dissolution and precipitation kinetics of sheet silicates. In A.F. White and S.L. Brantely, Eds., Chemical weathering rates of silicate minerals, p. 173–234. Mineralogical Society of America, Washington D.C.

Neder, R.B., Burghammer, M., Grasl, T., Schulz, H., Bram, A., and Fiedler, S. (1999) Refinement of the kaolinite structure from single-crystal synchrotron data. Clays and Clay Minerals, 47, 487–494.

O'Neil, J.R. (1986) Theoretical and experimental aspects of isotopic fractionation. In J.W. Valley, J.H.P. Taylor, and J.R. O'Neil, Eds., Stable Isotopes in High Temperature Geological Processes, p. 1–40. Mineralogical Society of America, Washington, D.C.

Phillips, B.L., Casey, W.H., and Karlsson, M. (2000) Bonding and reactivity at oxide mineral surfaces from model aqueous complexes. Nature, 404, 379–382.

Savin, S.M. and Lee, M. (1988) Isotopic studies of phyllosilicates. In S.W. Bailey, Ed., Hydrous phyllosilicates (exclusive of micas), p. 189–223. Mineralogical Society of America, Washington, D.C.

Sohlberg, K., Pennycook, S.J., and Pantelides, S.T. (1999) Hydrogen and the structure of the transition aluminas. Journal of the American Chemical Society, 121, 7493–7499.

Sposito, G., Skipper, N.T., Sutton, R., Park, S.H., Soper, A.K., and Greathouse, J.A. (1999) Surface geochemistry of the clay minerals. Proceedings of National Academy of Science USA, 96, 3358–3364.

Stebbins, J.F., Zhao, P., Lee, S.K., and Cheng, X. (1999) Reactive Al–O–Al sites in a natural zeolite: triple-quantum oxygen-17 nuclear magnetic resonance. American Mineralogist, 84, 1680–1684.

Stebbins, J.F., Kroeker, S., Lee, S.K., and Kiczenski, T.J. (2000) Quantification of five- and six-coordinated aluminum ions in aluminosilicate and fluoride-containing glasses by high-field, high-resolution Al-27 NMR. Journal of Non-Crystalline Solids, 275, 1–6.

Stoffregen, R. (1996) Numerical simulation of mineral-water isotope exchange via Ostwald ripening. American Journal of Sciences, 296, 908–931.

Sverjensky, D.A. (1992) Linear free-energy relations for predicting dissolution rates of solids. Nature, 358, 310–313.

van Eck, E.R.H., Smith, M.E., and Kohn, S.C. (1999) Observation of hydroxyl groups by ^{17}O solid-state multiple quantum NMR in sol-gel produced silica. Solid State NMR, 15, 181–188.

Vermillion, K.E., Florian, P., and Grandinetti, P.J. (1998) Relationships between bridging oxygen O-17 quadrupolar coupling parameters and structure in alkali silicates. Journal of Chemical Physics, 108, 7274–7285.

Walter, T.H. and Oldfield, R. (1989) Magic angle spinning oxygen-17 NMR of aluminum oxides and hydroxides. Journal of Physical Chemistry, 93, 6744–6751.

Walter, T.H., Turner, G.L., and Oldfield, E. (1988) Oxygen-17 cross polarization NMR spectroscopy of inorganic solids. Journal of Magnetic Resonance, 76, 106–120.

Xiao, Y.T. and Lasaga, A.C. (1994) Ab Initio quantum mechanical studies of the kinetics and mechanisms of silicate dissolution: H^+ (H_3O^+) catalysis. Geochimica et Cosmochimica Acta, 58, 5379–5400.

Xu, Z. and Stebbins, J.F. (1998) Oxygen site exchange kinetics observed with solid state NMR in a natural zeolite. Geochimica et Cosmochimica Acta, 62, 1803–1809.

Xu, Z., Maekawa, H., Oglesby, J.V., and Stebbins, J.F. (1998) Oxygen speciation in hydrous silicate glasses—An oxygen-17 NMR study. Journal of the American Chemical Society, 120, 9894–9901.

Zhao, P., Neuhoff, P.S., and Stebbins, J.F. (2001) Comparison of FAM mixing to single-pulse mixing in O-17 3Q-and 5Q-MAS NMR of oxygen sites in zeolites. Chemical Physics Letters, 344, 325–332.

MANUSCRIPT RECEIVED MAY 27, 2002
MANUSCRIPT ACCEPTED NOVEMBER 1, 2002
MANUSCRIPT HANDLED BY SIMON KOHN